This paper is published as part of Faraday Discussions volume 140:

Electrocatalysis - Theory and Experiment at the Interface

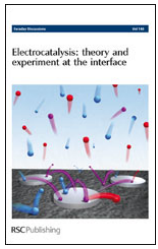

Preface

Preface
Andrea E. Russell, *Faraday Discuss.*, 2009
DOI: 10.1039/b814058h

Introductory Lecture

Electrocatalysis: theory and experiment at the interface
Marc T. M. Koper, *Faraday Discuss.*, 2009
DOI: 10.1039/b812859f

Papers

The role of anions in surface electrochemistry
D. V. Tripkovic, D. Strmcnik, D. van der Vliet, V. Stamenkovic and N. M. Markovic, *Faraday Discuss.*, 2009
DOI: 10.1039/b803714k

From ultra-high vacuum to the electrochemical interface: X-ray scattering studies of model electrocatalysts
Christopher A. Lucas, Michael Cormack, Mark E. Gallagher, Alexander Brownrigg, Paul Thompson, Ben Fowler, Yvonne Gründer, Jerome Roy, Vojislav Stamenković and Nenad M. Marković, *Faraday Discuss.*, 2009
DOI: 10.1039/b803523g

Surface dynamics at well-defined single crystal microfacetted Pt(111) electrodes: *in situ* optical studies
Iosif Fromondi and Daniel Scherson, *Faraday Discuss.*, 2009
DOI: 10.1039/b805040f

Bridging the gap between nanoparticles and single crystal surfaces
Payam Kaghazchi, Felice C. Simeone, Khaled A. Soliman, Ludwig A. Kibler and Timo Jacob, *Faraday Discuss.*, 2009
DOI: 10.1039/b802919a

Nanoparticle catalysts with high energy surfaces and enhanced activity synthesized by electrochemical method
Zhi-You Zhou, Na Tian, Zhi-Zhong Huang, De-Jun Chen and Shi-Gang Sun, *Faraday Discuss.*, 2009
DOI: 10.1039/b803716g

Discussion

General discussion
Faraday Discuss., 2009,
DOI: 10.1039/b814699n

Papers

Differential reactivity of Cu(111) and Cu(100) during nitrate reduction in acid electrolyte
Sang-Eun Bae and Andrew A. Gewirth, *Faraday Discuss.*, 2009
DOI: 10.1039/b803088j

Molecular structure at electrode/electrolyte solution interfaces related to electrocatalysis
Hidenori Noguchi, Tsubasa Okada and Kohei Uosaki, *Faraday Discuss.*, 2009
DOI: 10.1039/b803640c

A comparative *in situ* ^{195}Pt electrochemical-NMR investigation of PtRu nanoparticles supported on diverse carbon nanomaterials
Fatang Tan, Bingchen Du, Aaron L. Danberry, In-Su Park, Yung-Eun Sung and YuYe Tong, *Faraday Discuss.*, 2009
DOI: 10.1039/b803073a

Spectroelectrochemical flow cell with temperature control for investigation of electrocatalytic systems with surface-enhanced Raman spectroscopy
Bin Ren, Xiao-Bing Lian, Jian-Feng Li, Ping-Ping Fang, Qun-Ping Lai and Zhong-Qun Tian, *Faraday Discuss.*, 2009
DOI: 10.1039/b803366h

Mesoscopic mass transport effects in electrocatalytic processes
Y. E. Seidel, A. Schneider, Z. Jusys, B. Wickman, B. Kasemo and R. J. Behm, *Faraday Discuss.*, 2009
DOI: 10.1039/b806437g

Discussion

General discussion
Faraday Discuss., 2009,
DOI: 10.1039/b814700k

Papers

On the catalysis of the hydrogen oxidation
E. Santos, Kay Pötting and W. Schmickler, *Faraday Discuss.*, 2009
DOI: 10.1039/b802253d

Hydrogen evolution on nano-particulate transition metal sulfides
Jacob Bonde, Poul G. Moses, Thomas F. Jaramillo, Jens K. Nørskov and Ib Chorkendorff, *Faraday Discuss.*, 2009
DOI: 10.1039/b803857k

Influence of water on elementary reaction steps in electrocatalysis
Yoshihiro Gohda, Sebastian Schnur and Axel Groß, *Faraday Discuss.*, 2009
DOI: 10.1039/b802270d

Co-adsorbtion of Cu and Keggin type polytungstates on polycrystalline Pt: interplay of atomic and molecular UPD
Galina Tsirlina, Elena Mishina, Elena Timofeeva, Nobuko Tanimura, Nataliya Sherstyuk, Marina Borzenko, Seiichiro Nakabayashi and Oleg Petrii, *Faraday Discuss.*, 2009
DOI: 10.1039/b802556h

Aqueous-based synthesis of ruthenium–selenium catalyst for oxygen reduction reaction
Cyril Delacôte, Arman Bonakdarpour, Christina M. Johnston, Piotr Zelenay and Andrzej Wieckowski, *Faraday Discuss.*, 2009
DOI: 10.1039/b806377j

Size and composition distribution dynamics of alloy nanoparticle electrocatalysts probed by anomalous small angle X-ray scattering (ASAXS)
Chengfei Yu, Shirlaine Koh, Jennifer E. Leisch, Michael F. Toney and Peter Strasser, *Faraday Discuss.*, 2009
DOI: 10.1039/b801586d

Discussion

General discussion
Faraday Discuss., 2009,
DOI: 10.1039/b814701a

Papers

Efficient electrocatalytic oxygen reduction by the 'blue' copper oxidase, laccase, directly attached to chemically modified carbons
Christopher F. Blanford, Carina E. Foster, Rachel S. Heath and Fraser A. Armstrong, *Faraday Discuss.*, 2009
DOI: 10.1039/b808939f

Steady state oxygen reduction and cyclic voltammetry
Jan Rossmeisl, Gustav S. Karlberg, Thomas Jaramillo and Jens K. Nørskov, *Faraday Discuss.*, 2009
DOI: 10.1039/b802129e

Intrinsic kinetic equation for oxygen reduction reaction in acidic media: the double Tafel slope and fuel cell applications
Jia X. Wang, Francisco A. Uribe, Thomas E. Springer, Junliang Zhang and Radoslav R. Adzic, *Faraday Discuss.*, 2009
DOI: 10.1039/b802218f

A first principles comparison of the mechanism and site requirements for the electrocatalytic oxidation of methanol and formic acid over Pt
Matthew Neurock, Michael Janik and Andrzej Wieckowski, *Faraday Discuss.*, 2009
DOI: 10.1039/b804591g

Surface structure effects on the electrochemical oxidation of ethanol on platinum single crystal electrodes
Flavio Colmati, Germano Tremiliosi-Filho, Ernesto R. Gonzalez, Antonio Berná, Enrique Herrero and Juan M. Feliu, *Faraday Discuss.*, 2009
DOI: 10.1039/b802160k

Electro-oxidation of ethanol and acetaldehyde on platinum single-crystal electrodes
Stanley C. S. Lai and Marc T. M. Koper, *Faraday Discuss.*, 2009
DOI: 10.1039/b803711f

Discussion

General discussion
Faraday Discuss., 2009,
DOI: 10.1039/b814702g

Concluding remarks

All dressed up, but where to go? Concluding remarks for FD 140
David J. Schiffrin, *Faraday Discuss.*, 2009
DOI: 10.1039/b816481a

Spectroelectrochemical flow cell with temperature control for investigation of electrocatalytic systems with surface-enhanced Raman spectroscopy

Bin Ren,* Xiao-Bing Lian, Jian-Feng Li, Ping-Ping Fang, Qun-Ping Lai and Zhong-Qun Tian

Received 27th February 2008, Accepted 23rd April 2008
First published as an Advance Article on the web 21st August 2008
DOI: 10.1039/b803366h

We describe a method for investigating the reaction mechanism of fuel cell systems by designing a spectroelectrochemical cell with functions of temperature and flow control to mimic the reaction condition of fuel cell systems and utilizing Au core Pt shell (Au@Pt) nanoparticles to enhance the Raman signal of the surface species on the surface of electrocatalysts. The cell consists of three parts: a thin-layer spectroelectrochemical reaction chamber with an optical window for Raman measurement, the heating chamber right beneath the reaction chamber, and a long spiral flow channel to preheat the solution to the desired temperature and effectively exchange the solution. The temperature of the solution can be easily controlled from room temperature to 80 °C, and the flow rate can be as high as 945 μl s^{-1}. The temperature and flow control is demonstrated by monitoring the changes in the cyclic voltammograms and the Raman signals. By synthesizing Au@Pt nanoparticles and assembling them on a Pt substrate, we can significantly enhance the Raman signal of surface species on the Pt shell surface, which allows us to detect strong signal of CO as the dissociative product of formic acid as well as the intermediate species of the oxidation process. The further development and perspectives of using SERS to study the electrocatalytic systems are discussed.

Introduction

C1 molecules have attracted extensive attention in the research and development of fuel cells due to their special advantages such as abundant resources, easy storage and transportation, and high energy density.[1–5] In aid of optimizing the reaction condition and designing the electrocatalysts, various types of electrochemical methods and *in situ* and *ex situ* surface techniques, including NMR, DEMS, and IR spectroscopy, have been used to study the adsorption and reaction of C1 molecules on platinum group metals or their alloys.[6–12] Different mechanisms have been proposed to understand the phenomenon observed under different experimental conditions.

Among these methods, vibrational spectroscopic techniques manifest themselves with their special advantages in understanding the electrocatalytic mechanisms with the molecular level information. IR has been most widely applied to investigate

State Key Laboratory for Physical Chemistry of Solid Surfaces, College of Chemistry and Chemical Engineering, Department of Chemistry, Xiamen University, Xiamen, 36100, China. E-mail: bren@xmu.edu.cn; Fax: +86-592-2085349; Tel: +86-592-2186532

the electroxidation of methanol and formic acid on bi- and multi- component catalysts.[7,8] It can conveniently obtain the vibrational information in the high frequency region (higher than 1000 cm^{-1}) of the adsorbed species on single crystal surfaces, smooth electrode surfaces and the surfaces of low roughness. It has provided abundant valuable data for the identification of the adsorbed species on surfaces.[8–12] However, IR has its own limitations. For example, it is very difficult to obtain the information in the low frequency region reflecting the interaction between the substrate and the adsorbates unless a very strong light source, such as synchrotron, is used and it can normally only be applied to the surfaces of a very high reflectivity.

SERS is complementary to the IR in these aspects. It can be applied not only to the electrode surfaces of high roughness and low reflectivity that is very close to the practically used materials, but also to detect the vibrations reflecting the interaction between the substrate and adsorbates in the low frequency region.[13–17] These two unique features make SERS advantageous in the study of electrocatalytic systems. Previous SERS studies were mainly limited to Ag, Cu and Au surfaces. In the past 10 years, we have developed special surface preparation methods for generating SERS-active surfaces of transition metals and their alloys, including Pt, Pd, Rh and Pt–Ru, and performed electrochemical Raman study of the oxidation of carbon monoxide, methanol and formic acid on the surfaces.[13,14,18–20] We have demonstrated using SERS that the dual-path reaction mechanism and the bi-functional mechanism operates on Pt and Pt–Ru surfaces, respectively, during the oxidation of methanol.[21]

In parallel, Weaver's group developed a strategy to coat a transition-metal thin layer over SERS-active Au substrates to improve the SERS detection sensitivity of the surface species on transition-metal surfaces. This strategy allowed them to study various electrocatalytic systems, including the adsorption or dissociative adsorption and electrooxidation of CO, methanol, and formic acid.[15,22,23]

It should be pointed out that most of these previous studies, especially in the case of SERS, were performed at room temperature and in a static solution. However, in real fuel cell systems, the reaction normally takes place at a high temperature (*ca.* 80 °C) and under a flow condition.[24] Therefore, in order to understand the reaction mechanisms in the fuel cell systems, it is important to perform the SERS studies under a similar condition to the real reaction.

It is not difficult for an electrochemical cell to have a function of temperature and flow control. But in a spectroelectrochemical system, the detection sensitivity becomes the major concern as there are only a monolayer species at the surface.[25] It becomes a challenge to include the temperature and flow controls while maintaining a good potential control over the electrochemical system and allowing an efficient detection of the spectral signal.

In 2001, Weaver's group reported a thin layer flow cell to allow a rapid replacement of solution in 1 s, allowing study of electrochemical processes down to this time scale by means of temporal SERS sequences.[26] From 2000, our group have also concentrated on developing new types of cell for *in situ* SERS studies. We reported a three-phase Raman cell that can work under the conditions of both the solid/liquid interface with a potential control and the solid/gas interface with a convenient gas flow control.[19] This cell was further applied to solid/liquid/gas interfaces with a convenient exchange of the solution and gas flow. We found that the dissociative adsorbed CO generated at the solid/liquid interface can migrate across the three-phase region to the solid/gas interface. In order to realize temperature control on these two types of Raman cells, the source solution has to be heated up in a separate chamber and pumped into the Raman cell for measurement. This design will on one hand complicate the experiment, and on the other hand lead to a significant drop of the solution temperature in the flow path to the cell.

In this work, we design a spectroelectrochemical flow cell with a convenient temperature control so that the room temperature electrolyte can be heated up after being purged inside the cell body. The temperature of the solution can be controlled from room temperature up to 80 °C by a thermocouple put right underneath

the working electrode. The flow rate of the electrolyte is controlled by changing the relative height of the source solution and the exhaust solution or the gas pressure of the source solution chamber. Electrochemical and SERS measurements are made to demonstrate the effectiveness of the temperature and flow control. In order to further enhance the surface Raman signal of the surface species on transition-metal surfaces, we ultilize a "borrowing SERS" strategy, which is to coat a very thin layer of Pt over a highly SERS-active Au nanoparticle core (Au@Pt) to produce 2 orders of magnitude enhancement over the normal electrochemically roughened pure Pt eletrode.

Experimental

Electrochemical cyclic voltammograms (CV) were recorded on a CHI631a electrochemical workstation. Raman spectra were obtained using a confocal microprobe Raman system (LabRam I, Jobin-Yvon). The excitation line was 632.8 nm from an external He–Ne laser. A 50× long working-length objective (8 mm) was used in the present experiment. The width of the slit was 200 μm and the diameter of the pinhole was 800 μm.

A polycrystalline Pt electrode with an exposed diameter of about 2 mm was used as the working electrode. The Pt electrode was prepared by melting a commercially available Pt rod with a purity of 99.99% and subsequently removing impurities concentrating on the electrode surface in a *regia aqua* solution After several rounds of melting and removing, the formed Pt sphere was inserted into a Teflon shroud. Then, the top part of the sphere was polished to obtain a mirror finish and leakage free Pt disk electrode. The counter and reference electrodes were a platinum ring and a saturated calomel electrode (SCE), respectively.

HCOOH, $K_4Fe(CN)_6$, $K_3Fe(CN)_6$, KCl used in this study were of analytical grade reagents. H_2SO_4 is guaranteed reagent grade. All solutions were prepared with Mill-Q water.

Results and discussion

Cell design

As mentioned above that most of previous spectroelectrochemical cells had a separate heating chamber to the cell to simplify the cell design. However, during the transportation of the high temperature solution in the very thin pipe to the cell, the temperature will drop significantly. So a temperature monitoring device, such as a thermocouple, has to be put in the cell. On the other hand, during the experiment, several setups have to be constructed together, which will lead to a difficulty in handling. To overcome these problems, we designed and fabricated a spectroelectrochemical flow cell with potential control.

Fig. 1 shows a scheme of the design of the cell. According to its function, the cell can be described in three parts: the spectroelectrochemical cell, the flow control, and the temperature control. The spectroelectrochemical cell part consists of, from top to bottom, the optical window, the cell body, the working electrode, the counter electrode, the reference electrode, and the reaction chamber to accommodate all the electrodes and the electrochemical reaction. Due to the special requirement of the Raman measurement and the flow efficiency, the reaction chamber has to be as small as possible. For example, to improve the detection sensitivity, the solution layer between the surface of the working electrode and the optical window has to be as thin as possible, for example, 0.5–0.7 mm, which produces a volume of the reaction chamber less than 30 μL. The flow rate of the cell was simply controlled by elevating the bottle containing the fresh source solution or by changing the gas pressure to produce a continuous solution flow rather than a pulse flow when a pump is used. In a flow cell, the pressure inside the cell will be higher than the atmospheric pressure. To avoid solution leakage, the connection between the quartz window,

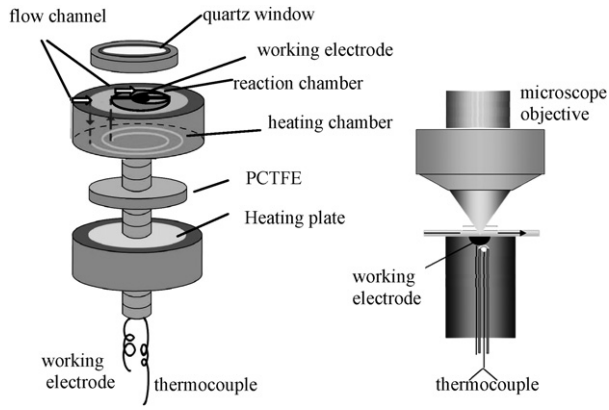

Fig. 1 The scheme of a spectroelectrochemical flow cell with temperature control, consisting of three major parts: the reaction chamber for the electrochemical control and Raman measurement, the flow channel to control the flow rate and heat exchange, and the temperature control unit with a heating plate and a thermocouple.

the working electrode and the reference electrode with the cell body were made with rubber O-rings. As the solution layer is very thin, it will be very difficult to purge the generated gas bubbles out of the cell body. To solve this problem, we designed the reaction chamber in an elliptic shape, and the working electrode is placed asymmetrically at one narrow end right facing the spiral outlet (or inlet of reaction chamber). Therefore, the outlet forms almost a V shape so that the bubbles can be squeezed out of it. The counter electrode was placed in the lower stream of the cell, so that the reaction products generated on the counter electrode will not contaminate the working electrode.

In the cell design, the most challenging part is the temperature control unit. It consists of a spiral channel, a PCTFE thin plate, a heater, and a supporting base. The spiral channel forms a close space by the PCTFE plate realized by using an O-ring. The solution is travelling from the outer spiral inlet to the central sprial outlet and further pushed up to the reaction chamber. The purpose of the spiral channel is to increase the length of the flow path to ensure a sufficient exchange of heat to reach the controlled temperature. The heating plate is also a self-designed unit, with a hole in the center for the working electrode to go through. The power of the heating plate can be adjusted by changing the applied voltage. The temperature is monitored with a thermcouple placed right underneath the Pt sphere working electrode. As Pt is a good heat conductor, the temperature difference between the surface of the working electrode and the sensing point of the thermocouple should be very small.

Demonstration of the temperature control

In a real electrocatalytic system, it is important to have an accurate control over the reaction temperature. For this purpose, we calibrated the temperature by simply using the intensity ratio of the anti-Stokes (I_{AS}) to Stokes (I_S) Raman signal intensities of the 520.6 cm^{-1} band of a silicon single crystal wafer. It is well known in Raman spectroscopy that the ratio depends on the temperature:[27]

$$\frac{I_{AS}}{I_S} = \left(\frac{\nu_0 + \nu_k}{\nu_0 - \nu_k}\right)^4 \exp\left(\frac{-1.4 \times \nu_k}{T}\right) \quad (1)$$

where ν_0, ν_k and T are the incident laser frequency, the Raman shift frequency, and the temperature, respectively. Therefore, if we measure the ratio, we can easily obtain the real temperature at the sample surface. The result is shown in Fig. 2.

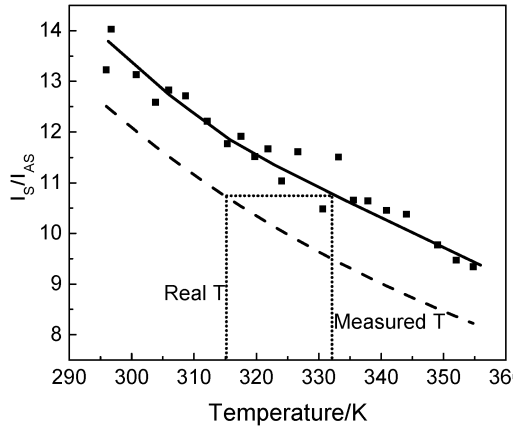

Fig. 2 The calibration curve of the cell temperature. The filled squares are the measured intensity ratio of the anti-Stokes to the Stokes bands of a silicon wafer using 1st phonon band at 520 cm^{-1}. The upper line is the fitting result of the measured experimental ratio and the dash line are the calculated ratio at the temperature of interest.

The dash line is the calculated value based on the eqn (1), the filled squares are the measured ratio. As the experimental temperature was read from the thermocouple, and the thermocouple was at a closer distance to the heating plate than the sample surface, the temperature obtained from the thermocouple will be slightly higher than the real value estimated from anti-Stokes to Stokes ratio, *i.e.*, the real temperature on the sample surface. The calculated curve and the experimental curve can serve as a working curve in the future experiment. For example, from the Raman measurement, we found a deviation of about 17 °C in the real temperature to the read temperature. So, in the future experiment, we can simply read the temperature from the thermocouple and, subtracting the difference read from the two curves, we can obtain the accurate temperature of the electrode surface.

To demonstrate the effect of temperature on the reaction of the electrocatalytic system, we used the oxidation of formic acid as a model system by monitoring the CV, and the result is shown in Fig. 3. It can be seen from the Figure that the reaction

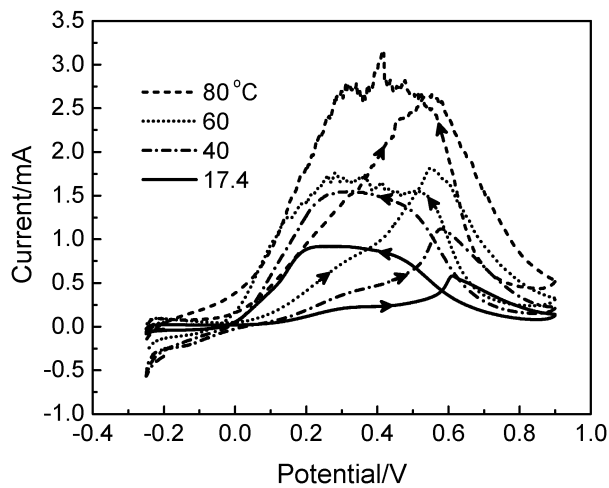

Fig. 3 Cyclic voltammograms of a Pt electrode at elevated temperatures as indicated in the Figure in the solution of 0.1 M HCOOH + 0.5 M H_2SO_4. The scan rate is 50 mV s^{-1}.

current increases progressively with the increasing temperature both in the positive and negative potential scan. The oxidation potential was also obviously negatively moved, indicating the oxidation reaction can take place more easily on the Pt surface. Furthermore, at temperatures higher than 60 °C, due to the vigorous oxidation of formic acid on the Pt surface, some noise on the CV curve can be found, which may be due to the formation of bubbles on the surface during the oxidation process. Another major difference is that the shape of the curve also changes quite significantly with the temperature, which may indicate a difference in the reaction process, especially at the lower potentials. The result demonstrates that we can easily control the temperature of the system by integrating the heating unit in the spectroelectrochemical cell body. It also demonstrates that it is necessary to control the reaction temperature in order to study the oxidation mechanism that may change with the temperature.

Demonstration of flow efficiency

In an electrocatalytic system, such as the oxidation of formic acid, the formic acid is rapidly oxidized on the Pt surface and produces CO_2 and other intermediate species or by-products. The existence of products on the surface may alter the condition on the Pt electrode surface and interfere the analysis of the reaction process or even lead to the complication of the reaction mechanism. Therefore, it is necessary to use a flow cell, especially to simplify the analysis of reaction mechanism.

A very important parameter for characterizing a flow cell is the flow efficiency, which can be reflected by monitoring the reaction current from the CV curves.[23] To simplify the analysis, we performed a flow rate dependent cyclic voltammetric study of $K_4Fe(CN)_6/K_3Fe(CN)_6$ redox system, and the result is shown in Fig. 4. The currents appearing at the positive potentials and negative potentials correspond to the oxidation and reduction of $K_4Fe(CN)_6$ and $K_3Fe(CN)_6$, respectively. It can be seen from the figure that the current increases progressively with the increasing flow rate. When the flow rate is slower than 45 μL s^{-1}, we can still observe the current

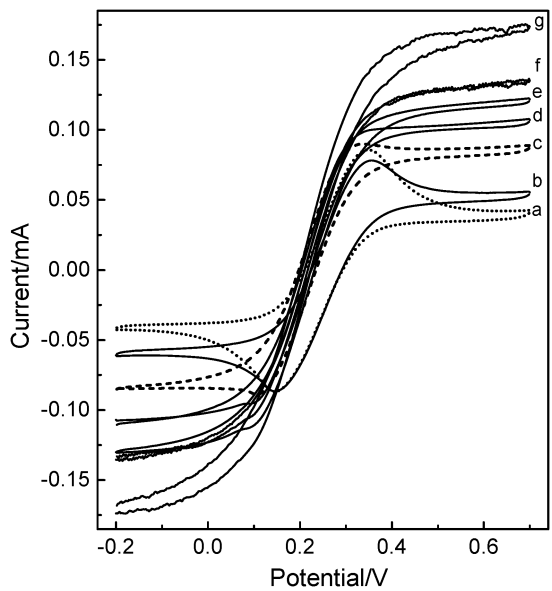

Fig. 4 Cyclic voltammograms of a Pt electrode obtained in a flow cell at different flow rates: (a) 17 μL s^{-1}; (b) 45 μL s^{-1}; (c) 127 μL s^{-1}; (d) 183 μL s^{-1}; (e) 274 μL s^{-1}; (f) 650 μL s^{-1}; (g) 945 μL s^{-1}. The solution is 1 mM $K_4Fe(CN)_6$ + 1 mM $K_3Fe(CN)_6$ + 0.1 M KCl. The scan rate is 100 mV s^{-1}.

peak indicating the diffusion controlled process. However, when the flow rate is higher than 127 μL s^{-1}, no peak was observed. Instead, we only see plateaus on both potential extremities. Further increase of the flow rate does not change the curve form too much, but a progressive increase in the plateau current indicated a forced convection process. The phenomenon is similar to the case of a rotating-disk electrode configuration. As has been stated above, the volume of the reaction chamber of the cell is only about 30 μL, we would expect the solution can be totally replaced at the flow rate of 45 μL s^{-1}. However, from Fig. 4 we find that a complete exchange of the solution might occur at a flow rate between 45 μL s^{-1} and 127 μL s^{-1}. This value is in accordance with the 4.4 ml s^{-1}, *i.e.* 73 μL s^{-1} reported by Weaver's group.[23] It demonstrates that we can easily achieve the effective solution exchange at the temperature controlled cell by simply changing the relative height of the source solution to the exhaust solution or the pressure in the source solution chamber. When the flow rate is controlled at a condition similar to the working flow of fuel cell systems at the desired temperature, we can mimic the reaction process of an electrocatalytic system.

Borrowing SERS strategy to enhance the detection sensitivity

From above, we have demonstrated that we can conveniently control the temperature and flow rate of the desired system by designing a proper spectroelectrochemical flow cell with integrated heating unit. Then to use the cell for providing molecular information using SERS, it is necessary to have a substrate that can provide sufficiently high detection sensitivity.

About 12 years ago, our group have demonstrated that we were able to obtain SERS from an electrochemically roughened Pt surface,[18] which make it possible to obtain SERS signal of some molecules with very weak SERS activities. We have been able to obtain SERS signals of oxidation and adsorption of the dissociative product (carbon monoxide) of methanol on Pt. However, we have not been able to obtain SERS signal of intermediate species due to the lack of sufficient sensitivity.

Recently, a borrowing SERS strategy has been proposed, which is to coat a thin layer of transition metals (such as Pt, Pd, Ni, Co) on a highly SERS-active Au nanoparticle core surface, forming a core–shell structure.[14,28–33] This kind of nanoparticles have the chemical properties of the shell materials (such as Pt) and can still benefit from the SERS enhancement of the Au core due to the long-range effect of the electromagnetic enhancement. By using this method, we have been able to obtain the very strong signals of pyridine, thiocyanide and carbon monoxide from such nanoparticle surfaces. It provides an enhancement about 2 orders of magnitude higher than that of pure transition-metal surfaces. The core–shell structure shows particular advantages in investigating the system with very weak signals.

The Au core Pt shell nanoparticles (denoted as Au@Pt) were prepared by the following method: first, Au nanoparticles with a diameter of 55 nm were synthesized following the Frens method, and the obtained nanoparticles were used as the core or seed. Then, to 30 ml solution containing the Au core, different amounts (to obtain different shell thickness) of 1 mM H_2PtCl_6 was added, and the mixture was heated up to 80 °C. Then, half the volume of 10 mM ascorbic acid to that of H_2PtCl_6 was slowly dropped into above mixtures through a syringe controlled by a step motor while stirring. The mixtures were then stirred for another 30 min to ensure a complete reduction of H_2PtCl_6. The color of the mixtures turned from red brown to dark brown, indicating formation of products. The core–shell structure and the control of the thickness has been well-documented in our previous paper.[14]

The Au@Pt nanoparticles sol was then centrifuged for three times to remove excess reactants and to obtain a clean surface. Then, 25 μL aliquot of the remaining sol was cast on a mechanically polished and electrochemically cleaned smooth Pt electrode, which was dried in a desiccator for 30 min. Such an electrode is ready for electrochemical or SERS measurements. Fig. 5(a) shows the SEM image of

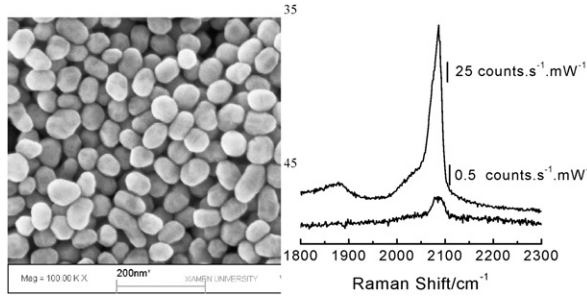

Fig. 5 (Left) SEM image of Au@Pt nanoparticles assembled on a Pt electrode(Au@Pt/Pt). (Right) SERS spectra of CO adsorbed on a roughened pure Pt electrode (bottom) and a Au@Pt/Pt electrode surface (top).

55 nm Au@0.7 nm Pt nanoparticles dispersed as a thin film on Pt (denoted as 55 nm Au@0.7 nm Pt/Pt), which shows a very uniform surface assembled with nanoparticles of very narrow size distribution. The surface shows a very uniform light golden color under daylight visible to naked eyes.

It should be noted that the Au@Pt nanoparticles shows very good SERS activity over a pure Pt electrode. To examine the SERS activity of the Au@Pt/Pt electrode, we carried out a comparative experiment on the electrochemically roughened Pt electrode and 55 nm Au@0.7 nm Pt/Pt using CO as the probe molecule. The result is shown in Fig. 5(b). The band at about 2086 cm^{-1} is due to the on-top adsorbed CO and that at about 1880 cm^{-1} is from the bridge-bound CO, as well recognized according to the results obtained in a previous SERS study[34] and IR spectroscopy.[35] By comparing the spectral intensity, we further found that the SERS signal from the 55 nm Au@0.7 nm Pt/Pt is much more intense, about 50 fold, than the pure massive Pt electrode and the bridge-bound CO can be clearly identified. The absolute height of the band is meaningless as the data acquisition time and power is different. In the former, a shorter time and a lower laser power was used, but the intensity is much higher than the latter. This result convincingly demonstrates that by using a core–shell strategy, we could dramatically enhance the detection sensitivity of the electrocatalytic system.

Investigation of the electrocatalytic system—CO and formic acid oxidation on Au@Pt/Pt electrode surfaces

Since formic acid is attracting increasing interest in using as a fuel, we use the electrooxidation of formic acid on the Au@Pt/Pt surface to demonstrate the function of our cell. Fig. 6 shows the SERS spectra obtained on the Au@Pt nanoparticles surface when the electrode potential was changed from negative to positive values at 40 °C. Similar to case of the CO system, we observed two bands at 2057 and 495 cm^{-1}, which can be routinely assigned to CO and Pt–C stretch of the on-top CO.[13,34] Compared with the case of CO, we find the frequency of the CO band is lower than the pure CO case, and the Pt–C band is higher. This difference can be explained by a lower CO coverage on the surface, as there may exist steric resistance during the dissociative adsorption, *i.e.*, the dissociation of formic acid to CO needs more than one surface Pt atom.[21,35,36] The intensity increases with the positive movement of the electrode potential up to 0.1 V, which can be understood by the restructuring of the surface CO. Further positive movement of the electrode potential leads to the oxidation of CO, whereas a significant increase of the SERS signal in the frequency region of 1100 to 1650 cm^{-1}.

Our control experiment in the 0.5 M H_2SO_4 solution without formic acid only shows a very weak SERS signal in this region, most possibly from the very trace

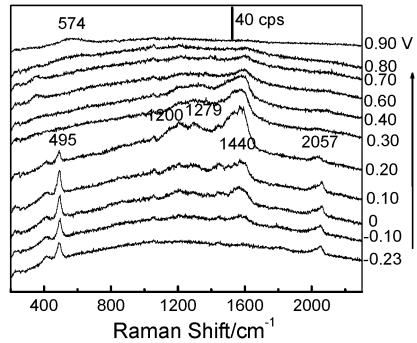

Fig. 6 SERS spectra obtained on a Au@Pt/Pt electrode in a solution containing 0.1 M HCOOH and 0.5 M H_2SO_4 at 40 °C. The acquisition time is 5 s.

amount of citrate left from the synthesizing process. It should be especially noted that the Au@Pt nanoparticles have been cleaned by centrifugation three times and water rinsing before assembly. Furthermore, after the nanoparticles were assembled on the surface, the electrode was further kept at a negative potential of −1.0 V to repel the contaminants from the surface and then the solution was changed to a fresh one. These efforts are to eliminate as much as possible the interference of contaminants. The comparative experiment may lead to a conclusion that the signal observed in frequency region of 1100 to 1650 cm^{-1} may have a combined contribution of intermediate species during the oxidation of formic acid and the trace amount of citrate. At present, it is still difficult to have a good assignment of the observed SERS signal in this region. The spectra were obtained with an integration time of 5 s and at a shorter intergration time, the spectra show a fluctuation character. A combination of these fluctuation feature leads to several broad bands in this region. Apparently, we need more experimental data to reach a statistic conclusion of the intermediate species.

It should also be pointed out that we have no evidence to exclude the possibility that the minor amount of impurities from formic acid may also be adsorbed on the surface to contribute to the signal, which also needs further investigation.

Conclusions and future development

A spectroelectrochemical cell with integrated functions of flow and temperature control was designed and fabricated. The electrochemical cyclic voltammetric results indicates that the flow rate can be effectively controlled from 0 to 945 μl s^{-1}, and the temperature can be controlled from room temperature up to 80 °C. The temperature of the electrode was calibrated by using the intensity ratio of Stokes to the anti-Stokes Raman bands, which is slightly lower than the temperature read from the thermal couple placed underneath the working electrode. By synthesizing Au core Pt shell nanoparticles, the SERS activity of Au can be borrowed to enhance the SERS activity of the Pt shell, so that the SERS signal of surface species can be significantly enhanced. It allows us to obtain an intense SERS signal of CO at the Au@Pt/Pt electrode surface in comparison with the pure Pt electrode surface. The cell was further used to study the electrooxidation of formic acid and the dissociative adsorption product, CO, of formic acid was detected. The control experiment demonstrates that the signal obtained in the region from 1100 to 1650 cm^{-1} may have a contribution from the intermediate species.

To further develop the Raman flow cell with variable temperature into a general technique for electrochemistry, there is still space to further improve the design and the substrate considering the following points.

First, the reaction chamber can be further minimized, so that the solution exchange can be more efficient, and the detection sensitivity of Raman measurement can be further improved. This can be done by thinning the inlet and outlet of the cell and by designing a special type of counter electrode.

Second, by using a special type of pump, so that the flow control can be integrated into the cell body. Thereafter, it is not necessary to have a flow pipe, which may increase the convenience of the experiment.

Third, since the nanoparticles were synthesized by chemical reduction method using citrate, it is inevitable that the surface will be covered with some organic contaminants. Although we have been using centrifugation or a hydrogen bubbling method to clean or desorb the contaminants, we still can not absolutely get rid of the contaminants at the present stage. It will be important to find a method to obtain contaminant free highly SERS-active substrates.

Four, in the present study, the Au core was completely covered by a Pt shell. It has been reported that small Au clusters may be good catalysts for the oxidation of CO. Therefore, if we reduce the amount of Pt so that submonolayer of Pt was formed on the Au surface, then the partial exposed Au substrate with the Pt surrounding may be good electrocatalysts. In addition, when the intermediate species are produced on the Pt surface, the intermediate species can diffuse to the Au surface with the highest enhancement, hopefully allowing detection the intermediate species that are very important for understanding the electrooxidation mechanisms.

Acknowledgements

The authors acknowledge the financial support by Natural Science Foundation of China and the Ministry of Science and Technology of China (20433040 and 20673086), the Ministry of Education of China(NCET-05-0564) and Fok Ying Tung Foundation (101015).

References

1 R. Parsons and T. Van der Noot, *J. Electroanal. Chem.*, 1988, **257**, 7.
2 S. Wasmus and A. Kuver, *J. Electroanal. Chem.*, 1999, **461**, 14.
3 B. Beden, C. Lamy and J.-M. Leger, in *Modern Aspects of Electrochemistry*, ed. J. O'M. Bockris, B. E. Conway and R. E. White, Plenum, New York, 1992, 22, p. 97.
4 K. A. Friedrich, K.-P. Geyzers, U. Linke, U. Stimming and J. Stumper, *J. Electroanal. Chem.*, 1996, **402**, 123.
5 A. Hamnett, in *Interfacial Electrochemistry*, ed. A. Wieckowski, Marcel Dekker, New York, 1999, 843.
6 Y. Y. Tong, A. Wieckowski and E. Oldfield, *J. Phys. Chem. B*, 2002, **106**, 2434.
7 H. Wang and H. Baltruschat, *J. Phys. Chem. C*, 2007, **111**, 7038.
8 J. M. Leger, S. Rousseau, C. Coutanceau, F. Hahn and C. Lamy, *Electrochim. Acta*, 2005, **50**, 5118.
9 Y. X. Chen, S. Ye, M. Heinen, Z. Jusys, M. Osawa and R. J. Behm, *J. Phys. Chem. B*, 2006, **110**, 9534.
10 D. Kardash and C. Korzeniewski, *Langmuir*, 2000, **16**, 8419.
11 N. Tian, Z. Y. Zhou, S. G. Sun, Y. Ding and Z. L. Wang, *Science*, 2007, **316**, 732.
12 S. Park, A. Wieckowski and M. J. Weaver, *J. Am. Chem. Soc.*, 2003, **125**, 2282–2290.
13 Z. Q. Tian, B. Ren and D. Y. Wu, *J. Phys. Chem. B*, 2002, **106**, 9463.
14 Z. Q. Tian, B. Ren, J. F. Li and Z. L. Yang, *Chem. Commun.*, 2007, 3514.
15 M. J. Weaver, S. Z. Zou and H. Y. H. Chan, *Anal. Chem.*, 2000, **72**, 38A.
16 R. L. Birke, T. Lu and J. R. Lombardi, in *Techniques for Characterization of Electrodes and Electrochemical Processes*, ed. R. Varma and J. R. Selman, John Wiley, New York, 1991, 211.
17 B. Pettinger, in *Adsorption at Electrode Surface*, ed. J. Lipkowski and P. N. Ross, VCH, New York, 1992, 285.
18 Z. Q. Tian, B. Ren and B. W. Mao, *J. Phys. Chem. B*, 1997, **101**, 1338.
19 B. Ren, X. F. Lin, J. W. Yan, B. W. Mao and Z. Q. Tian, *J. Phys. Chem. B*, 2003, **107**, 899.
20 Z. Liu, Z. L. Yang, L. Cui, B. Ren and Z. Q. Tian, *J. Phys. Chem. C*, 2007, **111**, 1770–1775.

21 C. X. She, J. Xiang, B. Ren, Q. L. Zhong, X. C. Wang and Z. Q. Tian, *J. Korean Electrochem. Soc.*, 2002, **5**, 221.
22 S. Park, Y. Xie and M. J. Weaver, *Langmuir*, 2002, **18**, 5792.
23 H. Luo and M. J. Weaver, *J. Electroanal. Chem.*, 2001, **501**, 141.
24 S. K. Kamarudin, W. R. W. Daud, S. L. Ho and U. A. Hasran, *J. Power Sources*, 2007, **163**, 743.
25 B. Ren, X. F. Lin, Y. X. Jiang, P. G. Cao, Y. Xie, Q. J. Huang and Z. Q. Tian, *Appl. Spectrosc.*, 2003, **57**, 419.
26 B. Ren, L. Cui, X. F. Lin and Z. Q. Tian, *Chem. Phys. Lett.*, 2003, **376**, 130.
27 G. I. Pangilinan and Y. M. Gupta, *Appl. Phys. Lett.*, 1997, **70**, 967.
28 Y. X. Jiang, J. F. Li, D. Y. Wu, Z. L. Yang, B. Ren, J. W. Hu, Y. L. Chow and Z. Q. Tian, *Chem. Commun.*, 2007, 4608.
29 B. Zhang, J. F. Li, Q. L. Zhong, B. Ren, Z. Q. Tian and S. Z. Zou, *Langmuir*, 2005, **21**, 7449.
30 J. F. Li, Z. L. Yang, B. Ren, G. K. Liu, P. P. Fang, Y. X. Jiang, D. Y. Wu and Z. Q. Tian, *Langmuir*, 2006, **22**, 10372.
31 J. W. Hu, Y. Zhang, J. F. Li, Z. Liu, B. Ren, S. G. Sun, Z. Q. Tian and T. Lian, *Chem. Phys. Lett.*, 2005, **408**, 354.
32 J. W. Hu, J. F. Li, B. Ren, D. Y. Wu, S. G. Sun and Z. Q. Tian, *J. Phys. Chem. C*, 2007, **111**, 1105.
33 S. Kumar and S. Z. Zou, *Langmuir*, 2007, **23**, 7365.
34 B. Ren, X. Q. Li, C. X. She, D. Y. Wu and Z. Q. Tian, *Electrochim. Acta*, 2000, **46**, 193.
35 Y. Y. Yang, S. G. Sun, Y. J. Gu, Z. Y. Zhou and C. H. Zhen, *Electrochim. Acta*, 2001, **46**, 4339.
36 Q. L. Zhong, P. Huang, B. Zhang, X. Y. Yang, Y. M. Ding, H. H. Zhou, B. Ren and Z. Q. Tian, *Acta Phys. Chim. Sin.*, 2006, **22**, 291.